NTU Journal of Engineering and Technology (ICSDT2025) special issue
DOI: https://doi.org/10.56286/ntujet.icsdt2025

IRAQI Academic Scientific Journals

P-ISSN: 2788-9971 E-ISSN: 2788-998X
NTU Journal of Engineering and Technology
Available online at: https://journals.ntu.edu.iq/index.php/NTU-JET/index

Enhancing Alzheimer's Disease Classification by Employing Deep Learning and Optimization

Nawzt Sadiq Jaafar Al-Bayati[1,2], Raid Rafi Omar Al-Nima[3]
[1]Technical Engineering College / Mosul, Northern Technical University (NTU), Mosul, Iraq,
[2]Vocational Education Department, Directorate of Ninawa Education, Ministry of Education, Mosul, Iraq,
[3]Technical Engineering College for Computer and Artificial Intelligence / Mosul, Northern Technical University, Mosul, Iraq
nawzt.sadek@ntu.edu.iq , raidrafi1@gmail.com.

Article Informations

Received: 15-03- 2025,
Accepted: 28-04-2025,
Published online: 01-03-2026

Corresponding author:
Name: Nawzt Sadiq Jaafar Al-Bayati
Affiliation: Northern Technical University
Email: nawzt.sadek@ntu.edu.iq

Key Words:
Alzheimer's disease,
classification,
Deep Learning,
optimization,
Convolutional Neural Network.

A B S T R A C T

Alzheimer's Disease (AD) is a progressive neurological disorder that leads to the deterioration of memory and cognitive abilities due to damage brain's nerve cells. Deep Learning (DL) techniques can provide effective AD classification by using medical imaging data. In this study, a DL technique based on Convolutional Neural Networks (CNN) is established. Keras-Tuner Optimization (KTO) is applied since it is difficult to propose a CNN with the suitable architecture. The aim of the proposed Optimized CNN (OCNN) model is to classify AD into four groups Mild Dementia (MD), Moderate Dementia (MoD), Non-Dementia (ND), and Very Mild Dementia (VMD). Two datasets are utilized here namely: Best Alzheimer Magnetic Resonance Imaging (BA-MRI) and Alzheimer's Disease Magnetic Resonance Imaging (AD-MRI). The Kaggle platform is the source and collection point for both datasets. After extensive implementations and OCNN models training, high classification accuracies of 92.44% and 93.17% are achieved for the AD-MRI and BA-MRI datasets, respectively.

THIS IS AN OPEN ACCESS ARTICLE UNDER THE CC BY LICENSE:
https://creativecommons.org/licenses/by/4.0/

1. Introduction

A gradual decline of memory and mental abilities is a feature of Alzheimer's Disease (AD), a neurological disorder and perhaps the most frequent kind of dementia in the elderly [1], Typically, the process starts out with a person's short-term memory deteriorating [2]. which in turn affects their capacity to recall commonplace events.

Dysfunction in thinking, speaking, and interacting with others is a symptom, as are changes in behavior and traits of character as the disease advances [3]. Proteins tau and beta-amyloid contribute to the development of AD. Beta-amyloid accumulates in the brain, forming plaques that disrupt connections between neurons, while tau protein leads to neuronal death and degeneration [4]. Beyond biological factors, environmental influences like lifestyle and nutrition play a crucial role in modulating the risk of developing AD [5]. Fig. 1 simulates healthy brain from AD and unhealthy brain with advanced AD [6].

The development of AD is influenced by environmental, genetic, and age-related factors. The current study aims to understand the causes of the disease and develop treatment plans, as the ongoing need for care places a significant psychological burden on both patients and caregivers [7]. Thus, understanding the stages of the condition and its impact on individuals and caretakers is crucial for awareness and treatment efforts [8].

This research seeks to categories AD) into its distinct stages: Mild Dementia (MD), Moderate Dementia (MoD), Non-Dementia (ND), and Very Mild Dementia (VMD). Our research contributes in constructing a Convolutional Neural Network (CNN) by employing Keras-Tuner Optimization (KTO). The proposed Optimized CNN (OCNN) model is able to enhance the diagnosis and classification of various stages of AD, ranging from no dementia to mild AD.

The rest sections of this paper are laid out as follows: Section 2 provides the literature review, Section 3 illustrates the proposed OCNN approach, Section 4 describes the two employed datasets and discusses the experimental results, and Section 5 provides the conclusion of the study.

2. Literature Review

A collection of previous studies that have explored the topic of Alzheimer can be presented as follows:

In 2013, Dyrba et al. demonstrated that machine learning algorithms enable accurate classification of Diffusion Tensor Imaging (DTI) data in spite of varying Magnetic Resonance Imaging (MRI) devices.

DTI metrics such as Fractional Anisotropy (FA) and Mean Diffusivity (MD), along with gray and white matter density maps from anatomical MRI, were used in the classification process. Support Vector Machine (SVM) and Naïve Bayes (NB) algorithms were employed, and two cross-validation methods were applied namely pooled cross-validation and scanner-specific cross-validation. An accuracy of 80% was achieved for SVM with FA and 83% with MD. NB accuracies were ranged from 68% to 75% [9].

In 2014, Sampath and Saradha highlighted the effectiveness of using an Adaptive Neuro Fuzzy Inference System (ANFIS) to classify AD stages. K-means clustering was applied for segmentation and Gray Level Co-occurrence Matrix (GLCM) was used for feature extraction. MRI data for 150 subjects from the AD Neuroimaging Initiative (ADNI) dataset were analyzed. The subjects were categorized into Normal Controls (NC), Mild Cognitive Impairment (MCI) and AD. The results were compared between SVM and ANFIS classifiers. A higher accuracy of 88% was attained by ANFIS compared to the accuracy of 77.34% which was obtained by SVM [10].

In 2015, Demirhan et al. improved the accuracy of Alzheimer's classification by using feature selection techniques. Fractional anisotropy maps from the images were analyzed. Furthermore, averages in elliptical Region of Interest (ROI) and different voxel maps in elliptical fibers were used to drive SVM. The Relief Feature (ReliefF) algorithm was also employed to identify the most discriminative voxels in elliptical fibers. The total data used in this work was comprised of 221 samples. The work here increased the classification accuracy for all tasks by up to 15% [11]. In 2016, Sarraf and Tofighi presented a method that utilized Convolutional Neural Network (CNN) to extract detailed features from brain images. Furthermore, LeNet-5 architecture was employed as an efficient classifier.

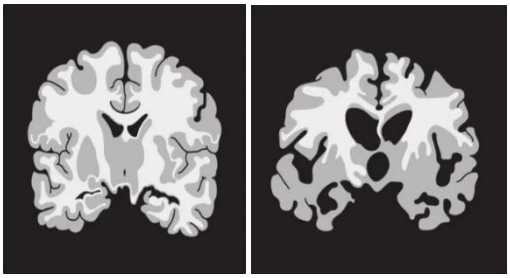

Fig. 1. Simulation of healthy and AD unhealthy brains, (a) healthy brain from AD and (b) unhealthy brain with advanced AD.

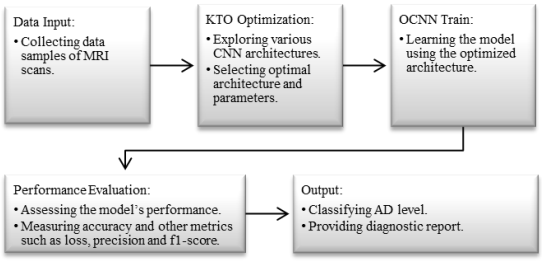

Fig. 1. Block diagram of the proposed OCNN model.

It was shown that the shift and scale-invariant features extracted by CNN followed by a deep learning classification such as LeNet-5 or Google Network (GoogleNet) could be exploited for more complex predictions. The dataset here, sourced from ADNI, included structural MRI images for 302 individuals over the age of 75. It comprised of 211 Alzheimer's patients and 91 non-Alzheimer's persons. was classified with an accuracy of 98.84% [12].

In 2017, Hon and Khan suggested a strategy for the classification of AD using Transfer Learning (TL) with CNN architectures, including Visual Geometry Group of 16 (VGG16) layers and inception (version 4) networks. TL was utilized by leveraging pre-trained weights of the Image Network (ImageNet) dataset in order to reduce the need for a large training dataset. Image entropy was employed to identify the most informative slices of MRI data. OASIS dataset, which includes 6,400 MRI images from 200 individuals, was utilized. Classification accuracies of 92.3% and 96.25% were attained by VGG16 and inception, respectively [13].

In 2018, Islam and Zhang used Deep Convolutional Neural Network (DCNN) to diagnose AD by analyzing brain MRI data. Due to employing small data size, techniques such as data augmentation were utilized to improve the performance. Data from OASIS cohort were used, which included 416 MRIs of individuals aged 18 to 96 years, with focusing on patients who are older than 60 years. Different stages of AD were classified with the successful accuracy of 93.18% [14].

In 2019, Razavi et al. offered an intelligent AD diagnosis system using unsupervised feature learning. Sparser filtering was utilized to extract important features and reduced the influence of unhelpful features. Softmax regression was exploited for classification. The employed dataset of ADNI included 202 samples for the ages between 55 and 89 years, it involved 150 patients and 52 healthy individuals. An accuracy of 94% was attained here [15].

In 2020, Mahajan et al. provided an overview of how machine learning techniques can improve the accuracy of AD diagnosis. SVMs were utilized to distinguish patient categories, while ANNs were employed to mimic brain processing. Deep learning techniques like convolutional networks were reviewed for feature extraction from MRI and Positron Emission Tomography (PET) scans. Iterative-based feature selection techniques were used to ensure the classification efficiency. With this overview, the accuracy of diagnosis is significantly improved, verified, and validated [16].

In 2021, Mahendran et al. focused on improving the classification of AD by using a hybrid pipeline of gene selection and deep learning. Minimum Redundancy Maximum Relevance (MRMR) strategy was used to reduce the redundancy between features and increase the relevance to target classes. Particle Swarm Optimization (PSO) was applied as a wrapper method to select relevant genes, with the Ki-Men algorithm to improve the results. An autoencoder was used to reduce dimensionality and compress data without significant information loss. Improved Deep Belief Network (IDBN) was employed to classify individuals for with and without AD. To enhance the accuracy optimal parameters for the IDBN model were determined using the Bayesian Optimization (BO) technique. The data were from the Gene Expression Omnibus (GEO) dataset, it included 161 samples. A high accuracy of 95.09% was reached [17].

In 2022, Sethi et al. suggested a Computer-Aided Diagnosis (CAD) system for classifying AD using Two-Dimensional (2D) MRI slices. A hybrid model which combined CNN and SVM was proposed to boost the classification accuracy. MRI data were converted from Neuroimaging Informatics Technology Initiative (NIfTI) format into 2D slices in order to be used and analyzed. The middle slices from the extracted 2D images were chosen to ensure uniformity in the training and testing data. The ADNI dataset was exploited, it consisted of 1000 samples. An accuracy of 88% was attained here [18].

In 2023, Mohi et al. designed a comprehensive CNN model to classify different stages of AD based on MRI data. Processing techniques such as rebalancing, data expansion, and preprocessing were applied to ensure the quality of the data used in training. CNN models such as Mobile Network)MobileNet(, VGG16 and Residual Network of 50 (ResNet50) layers were used, and their performances were compared. Total of 2,900 MRI samples from ADNI were employed in this work The MobileNet model was improved, it obtained an accuracy of up to 96.6% [19].

In 2024, Chen et al. presented a classification technique based on the integration of multimodal data such as EEG, eye tracking and behavioral data to diagnose AD. Data augmentation method was implemented to enlarge the dataset. Extra Event-Related Potential Network (ERPNet) feature extraction layer was developed to extract multi-modal features. Domain Adversarial Neural Network (DANN) algorithm was utilized to improve the performance of diagnosis.

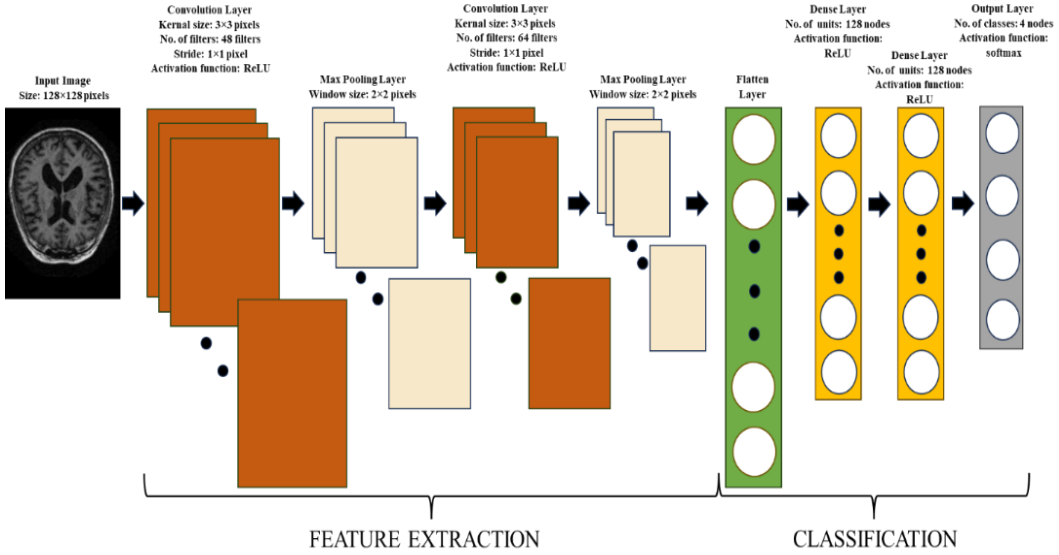

(a)

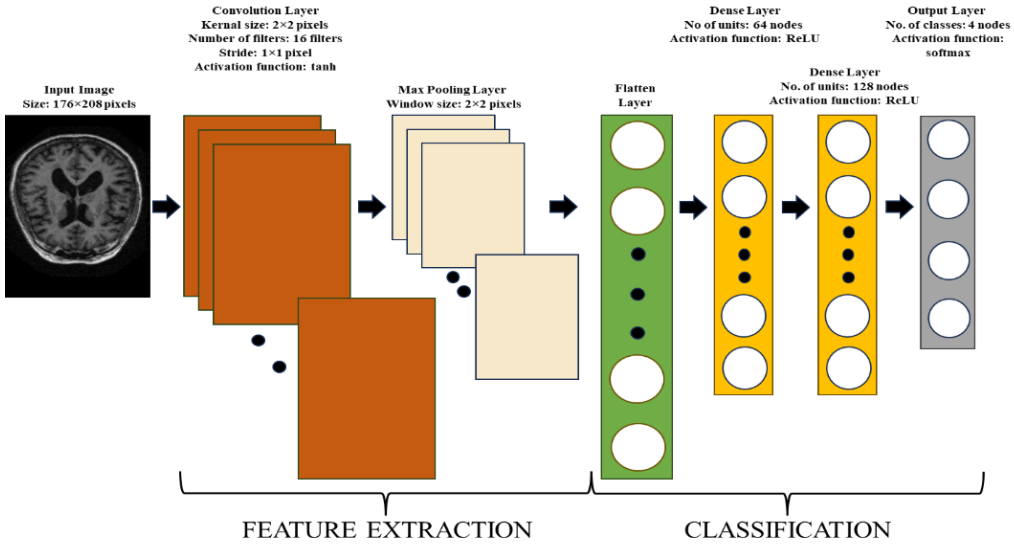

(b)

Fig. 3. Constructed architectures of the two deep learning models by using the proposed OCNN approach (a) a model of OCNN for BA-MRI dataset and (b) a model of OCNN for AD-MRI dataset.

Data from 69 participants were gathered at a hospital in China for this work. An average accuracy of 88.81% was reported [20].

To the best of our knowledge, there is no comprehensive study that has established a deep learning network by applying optimization for the case of AD classification. So, this study considers this by proposing the OCNN model, where CNN architectural and parametric are optimized. This study, in conclusion, makes a substantial addition to the field of artificial intelligence (AI), and it also includes the building of a neural network that may be utilized in other research projects, such as [21][22][23][24][25].

3. Methodology

3.1. Proposed OCNN

In this paper, we present a deep learning approach utilizing CNN architecture due to its well-known scalability [12][26]. CNNs are among the most prevalent types of deep learning and have demonstrated exceptional capabilities in addressing image data challenges [26]. The OCNN model was developed through the integration of CNN with the KTO, with the aim of diagnosing and classifying AD stages. The proposed model stands out on discovering a best CNN model by employing the KTO. In other words, KTO technique is employed to select the optimal architecture of the CNN network and efficiently tune its internal parameters.

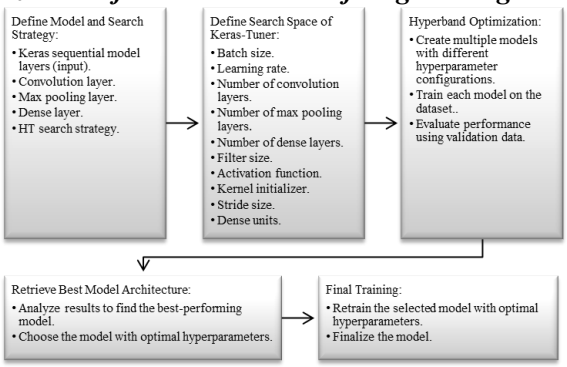

Fig. 4. Block diagram of KTO algorithm workflow.

Fig. 2 Illustrates a systematic and comprehensive workflow designed to enhance the accuracy and efficiency of Alzheimer's disease classification through the integration of advanced deep learning techniques.

This work is distinguished by integrating CNN with KTO, creating the OCNN approach, which enhances efficiency, accuracy, and performance in deep learning.

Established deep learning of OCNN, the CNN architecture discovered by the KTO, and given that we are working on two datasets result in constructing two distinct network architectures (models), each tailored to the specific characteristics of its respective dataset. Fig. 3 shows the constructed architectures of the two models by using the proposed OCNN approach.

In this paper, KTO is used to improve the performance of the CNN model by tuning the hyperparameters and choosing the optimal architecture based on a specific metric. This metric represents the goal that the system seeks to improve during the validation accuracy searching process. The accuracy equation can be given as:

$$Accur = \frac{Cp}{Tp} \times 100\% \qquad (1)$$

Where: Accur is the accuracy, Cp is the number of correct predictions and Tp is the total number of predictions [27][28].

3.2. KTO Algorithm

KTO advanced technique aims at enabling the optimal selection of hyperparameters for deep learning networks [29]. It allows changes and analysis of various topologies of networks to determine the best settings for enhancing performance.

Hyperband Technology (HT) speeds the finding of model architecture and its optimal hyperparameters. HT is an efficient optimization algorithm designed to accelerate the hyperparameter calibration process for machine learning models [29]. HT significantly reduces the time needed to find the correct hyperparameters by efficiently applying computational capacity [30].

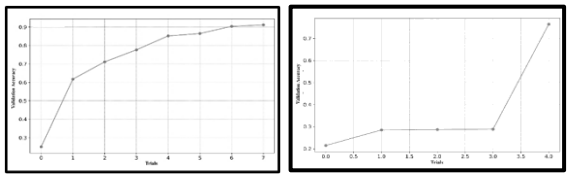

(a) (b)

Fig. 5. Efficacy of establishing OCNNs (a) for AD-MRI dataset and (b) for BA-MRI dataset.

Fig. 4 displays the KTO workflow as an efficient and iterative process designed to enhance model accuracy and reliability. It enables the deployment of a solution that is optimally configured through the application of advanced optimization techniques.The algorithm is initiated by defining a network that encompasses a series of tuning parameters [29]. These parameters include the batch size, learning rate, number of convolution layers, number of max pooling layers, number of dense layers, filter size, activation function, kernel initializer, stride size and dense units. They are known as the structural components of a network; various models are evaluated by the KTO in multiple experiments. In each round, the performance of each model is evaluated based on the validation accuracy. Well-performing models are retained, while poorly performing models are excluded. This continuous evaluation reduces the number of models in each round, leading to a more efficient allocation of resources.

Table 1. Configuration of OCNN architecture for AD-MRI dataset.

Layer Type	Kernal Size (pixels/nodes)	No. of Filters	Output Shape (pixels/nodes)	No. of Trainable Parameters
Convolution layer 1	3×3	16	174×103×16	448
Max pooling layer 1	2×2	---	87×51×16	0
Flatten layer	---	---	70992	0
Dense layer 1	64	---	64	4543552
Dense layer 2	128	---	128	8320
Dense layer 3	64	---	64	516
Total no. of parameters:				**4552836**
No. of trainable parameters:				**4552836**
No. of non-trainable parameters:				**0**

Table 2. Configuration of OCNN architecture for BA-MRI dataset.

Layer Type	Kernal Size (pixels/nodes)	No. of Filters	Output Shape (pixels/nodes)	No. of Trainable Parameters
Convolution Layer 1	3×3	48	63×63×48	480
Max Pooling Layer 1	2×2	---	31×31×48	0
Convolution Layer 2	3×3	64	29×29×64	27712
Max Pooling Layer 2	2×2	---	14×14×64	0
Flatten Layer	---	---	12544	0
Dense Layer 1	128	---	128	1605760
Dense Layer 2	128	---	128	16512
Dense Layer 3	4	---	4	512
Total no. of parameters:				**1,650,980**
No. of trainable parameters:				**1,650,980**
No. of non-trainable parameters:				**0**

The process continues until the model with the best performance is identified. After the search is complete, the most successful model can be retrieved. This step is crucial, as it helps improve the effectiveness of the final model and ensures accurate results.

Upon the completion of the KTO process, an integrated model is developed, representing the optimal configuration in terms of structure and internal parameters. The final model includes the specific layers necessary to achieve the best results. However, the exact structure of the model varies based on the used dataset.

3.3. Deep Learning network

Convolutional Neural Network (CNN) is a fundamental network in deep learning, it has specifically been designed to process data that comes in the form of interconnected matrices, such as images. It is exceptionally good at learning spatial patterns, making it extremely effective in computer vision tasks such as image classification and segmentation [26].

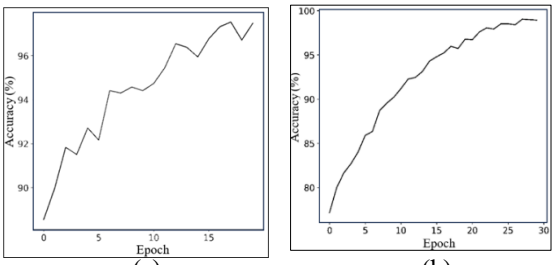

(a) (b)

Fig. 6. Training accuracy curves (a) for AD-MRI dataset and (b) for BA-MRI dataset.

The architecture of CNN can be composed of interconnected layers, beginning with the convolution layer, which is utilized to extract key features from the data. This is followed by the Rectified Linear Unit (ReLU) activation layer, adding nonlinearity to the model. In fact, convolution and ReLU can be considered as one layer. Subsequently, the max pooling layer is employed to reduce the dimensionality of the extracted information. The aforementioned layers may be repeated and they are all used to extract features from images. The subsequent layers are responsible for classification. These layers may contain a flattening layer, which prepares the data by converting it into a format suitable for input to the dense layer. The dense layer then adjusts the weights and biases through the learning process, ultimately passing the processed data to the final softmax layer. In the softmax layer, final decisions are made based on information received from the fully connected layer [31].

With its intricate architecture, a CNN can efficiently handle vast amounts of complex data, extracting patterns and features with precision. This capability translates into outstanding performance across various domains, especially in tasks like classification and image recognition. Below is an in-depth look at each layer, along with a mathematical equation illustrating the functionality of each layer.

The convolution layer plays a crucial role in extracting various features from an image. The convolution function can be represented by the following equation:

$$H_\alpha(p,q) = \sum_{m=1}^{M} \sum_{n=1}^{N} R(m,n) \times W(p-m, q-n) \quad (2)$$

Where: H(p,q) represents a calculated convolution, M and N respectively represents the width and height of the Two-Dimensional (2D) input image, and W(p-m ,q-n) represents a kernel value [32]. It is important to note that the value of H(p,q) is updated for a certain convolution (α) to be H_α (p,q), as multiple convolution layers may be constructed within the proposed OCNN.

Activation function can be exploited in the convolution layer of a CNN, such as ReLU and tanh. The ReLU is well known and it retains positive values and discards the negative ones,

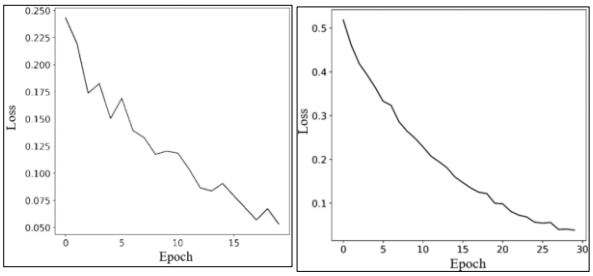

(a) (b)

Fig. 7. Training Loss curves (a) for AD-MRI dataset and (b) for BA-MRI dataset.

introducing non-linearity to the model. This function can be mathematically represented as follows:

$$Re_{\alpha}(x,y) = max(0, H_{\alpha}(p,q)) \quad (3)$$

Where: Re(x,y) represents a computed ReLU and max represents the maximum operation [33]. Also, Re(x,y) is updated for a certain ReLU (α) to be 〖Re〗_α (x,y), as multiple ReLUs may be utilized in the multiple convolution layers.

Subsequently, the pooling layer decreases the dimensions of previously analyzed vector. This layer can be one of two types: max pooling or average pooling [34]. Max pooling is often employed in CNNs. The general equation for the max pooling can be represented as follows:

$$P_{\beta}(k,l) = max(\mathbf{S}) \quad (4)$$

Where: P(k,l) represents a computed pooling and S is a small matrix part (or a window) in a previous 2D vector [34]. Similarly, P(k,l) is updated here for a certain pooling layer (β) to be P_β (k,l) as also multiple pooling layers can be established in the model.

A flatten layer converts a multi-dimensional vector into a One-Dimensional (1D) vector, preparing the data for the fully connected layer [35]. The flatten layer equation can be represented as follows:

$$Fl[i] = \sum_{g=1}^{h} \sum_{f=1}^{w} \sum_{r=1}^{e} T[g][f][r] \quad (5)$$

Where: Fl[i] represents the flattened output for the ith sample, T[g][f][r] refers to a value in a Three-Dimensional (3D) matrices, h, w and e are the numbers of rows, columns and channels, respectively. This layer encapsulates extracted features (feature maps), where they are transformed into a One-Dimensional (1D) vector suitable for processing in the next fully connected layer [35].

Dense layer (or fully connected layer) connects each neuron in the previous layer to all neurons in its layer. The fundamental equation describing the fully connected layer can be expressed as follows:

$$DE_{\gamma}(c) = B(c) + \sum_{z=1}^{b} \big(FW(c,z) \times N(z)\big) \quad (5)$$

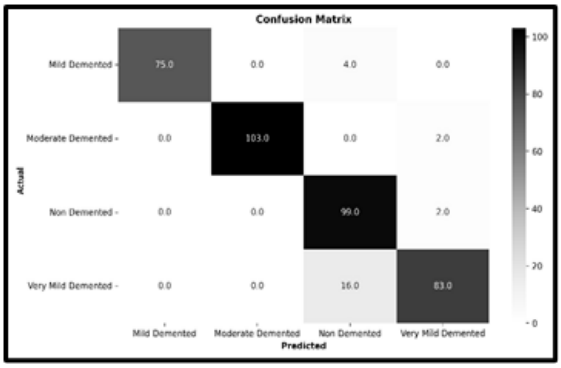

(a)

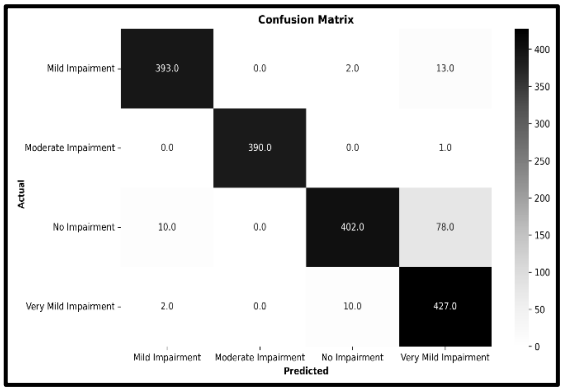

(b)

Fig. 8. Confusion matrices of the established OCNN models (a) for AD-MRI dataset and (b) for BA-MRI dataset

Where: DE(c) represents an output value of the fully connected layer, c represents the number of units (nodes) in the fully connected layer, B(c) represents a bias value, b represents the number of units in the previous layer, FW(c,z) represents a connection weight value between the pooling and fully connected layers, and N(z) represents the output value of a node in the previous layer [36]. Likewise, DE(c) is updated in this study for a certain pooling layer (□) to be 〖DE〗_□ (c) as multiple dense layers can be provided in the model too.

The output layer is finally used for the considered classification task. Essentially, this layer employs the softmax activation function. The fundamental equation here can be represented as follows:

$$SoM(C) = \frac{e^{DE_{\gamma}(c)}}{\sum_{lo=1}^{K} e^{DE_{\gamma}(lo)}} \quad (7)$$

Where: SoM(C) represents a calculated softmax value for class C and K is the number of classes [37][38].

4. Results and Discussion

4.1. Employed dataset

This work utilizes two MRI image datasets called the Best Alzheimer Magnetic Resonance

Imaging (BA-MRI) [39] and AD Magnetic Resonance Imaging (AD-MRI) [40]. Both datasets contain brain MRI images that have been analyzed by medical professionals, each image is of Joint Photographic Experts Group (JPG) format. The MRI images in any dataset are partitioned into four categories: Mild Dementia (MD), Moderate Dementia (MoD), Non-Dementia (ND) and Very Mild Dementia (VMD). Such partitioning has been exploited to be classified in this study.

4.1.1. BA-MRI dataset descriptions

This dataset includes a combination of genuine and synthetic axial MRI scans. The scans were obtained using MRI scanner of 1.5 Tesla with T1-weighted sequence. Each one of its images has a resolution of 128×128 pixels. All images have under-gone pre-processing to remove the skulls. In total, this dataset comprises of 11,519 images, where it includes 2,739 images for MD, 2,572 images for MoD, 3,200 images for ND, and 3,008 images for VMD.

4.1.2. AD-MRI dataset descriptions

This dataset comprises images captured using a Magnetic Resonance Imaging (MRI) scanner. The images have a resolution of 208 × 176 pixels. In total, this dataset includes 2,609 images, where it is divided as 646 images for MD, 637 images for MoD, 652 images for Non-Dementia (ND), and 674 images for VMD.

4.2. Experimental setup

All experiments were carried out using a computer, with the Google Colab environment utilized to process the two data groups. Each data group was initially partitioned into three distinct subsets for training, validation, and testing purposes, comprising 70%, 15%, and 15% of the data, respectively.

4.3. OCNN results and discussions

The proposed OCNN model is dynamically optimized for obtaining its architecture, including the number of convolution layers, number of dense layers, filter sizes, strides, and activation functions, specifically tailored for the utilized dataset through multiple trails. Such trails are conducted autonomously by the OCNN, with the validation accuracy being evaluated in each trial. The trails for both the AD-MRI and BA-MRI datasets are depicted in Fig. 5.

Upon the completion of the OCNN model experiments, the best model is retained. The resulting architectural configuration of OCNN models for both datasets are summarized in Table 1 and Table 2. Both tables also include all the determined parameters after using the KTO that contributes in constructing the optimal architectures for the proposed OCNN models.

Ultimately, the OCNN models are trained using the training sets and monitored using the validation sets. Remarkable results and high training accuracies have been achieved for both datasets, with 98.94% training accuracy for the BA-MRI and 97.47% training accuracy for the AD-MRI. Fig. 6 presents the training accuracy curves for both utilized datasets. Fig. 7 presents the training loss (error) curves for both employed datasets.

Following the training process, the validation accuracy of the model is recorded as 95.02% for the BA-MRI dataset and 95.05% for the AD-MRI dataset. These results highlight high performances of the OCNN models during the validation phase. To evaluate testing accuracies, one of the most prominent methods is the confusion matrix, which helps determining the numbers of correctly and incorrectly classified cases for each class.

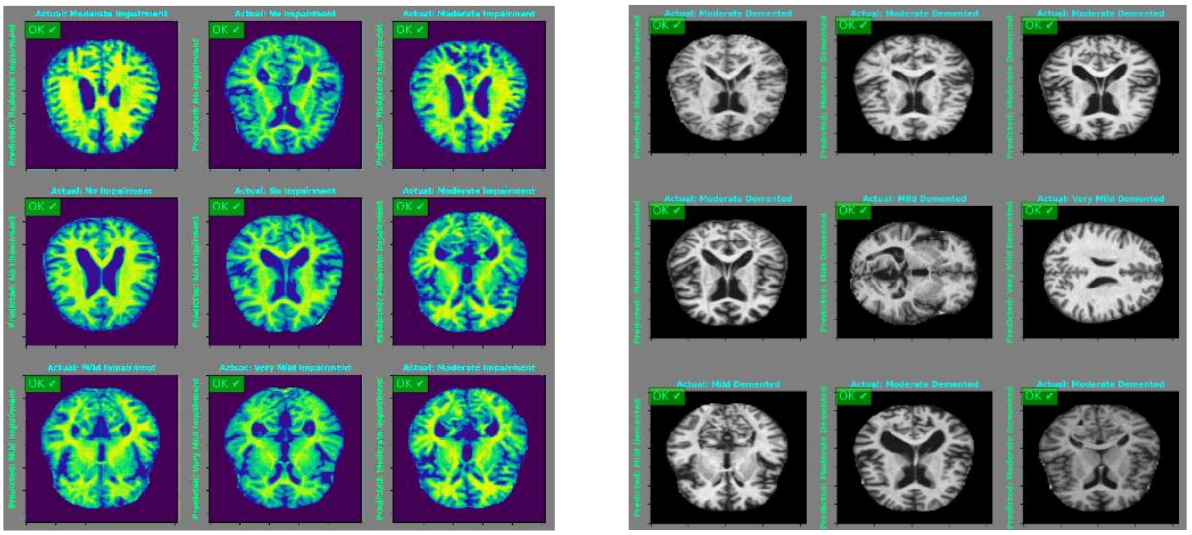

(a) (b)

Fig. 9. Simulating the mechanisms and performances of the diagnostic OCNN models in classifying between various AD categories (a) for BA-MRI dataset and (b) for AD-MRI dataset

Error! Reference source not found. presents the confusion matrices of testing the established OCNN models for both employed datasets, showing the relationships between the actual and predicted cases for each class. It is noteworthy that the proposed models achieve excellent overall testing accuracies. Specifically, the overall testing accuracy of 92.44% is recorded for the AD-MRI dataset and the overall testing accuracy of 93.17% is benchmarked for the BA-MRI dataset.

Several key metrics are derived from the confusion matrix to assess the model's performance, including the precision, recall and f1-score. Their results are found as 95.2%, 99.4% and 97.3% for the precision, recall and f1-score, respectively. Such results show high performance and acceptability.

Fig. 9 simulates the mechanisms and performances of the OCNN models in classifying between various categories of AD. The visual comparisons between actual and predicted classes emphasize the model's capabilities in classifying AD levels.

Our proposed OCNN has several unique characteristics, the most prominent of which is that it combines between KTO and CNN to provide the best-established architecture with parameters. In addition, it has been tested on two MRI datasets and showed significant results in predicting the stages of AD, making it a reliable decision support for doctors in their diagnosing task. the validation ensures the OCNN model's applicability outside controlled conditions by testing its performance on diverse clinical datasets. This process evaluates the model's robustness, adaptability to real-world scenarios, and its potential to aid medical diagnosis effectively. For real world validation, OCNN model's applicability has been approved by testing its performance with diverse clinical datasets. This process evaluates the model's robustness, adaptability to real-world scenarios and potential to aid medical diagnosis effectively.

The limitations of the study encompass the substantial computational demands
associated with KTO, as well as the challenges posed by the extensive computational operations required for this type of optimization. Reliance on a predefined searching space, sensitivity to data quality and distribution, and limitation in dynamic data can also be noted.

This study highlights the capabilities of the OCNN model in accurately classifying AD, contributing to early diagnosis and precise identification of disease stages. The findings emphasize the significance of artificial intelligence in clinical applications, such as alerting the patient's family or physician in case of emergencies. Moreover, the study paves the way for similar research on other neurological disorders, fostering advancements in diagnostics and treatment strategies.

5. Conclusion

In this paper, we proposed a hybrid technique that has the ability to establish an efficient deep learning network by applying effective optimization. That is, a proposed OCNN was well structured by combining between CNN and KTO. The core idea behind this integration is that KTO was exploited here for optimizing the optimal parameters and architecture of CNN, aiming to classify MRI brain images of AD into various stages or levels. The established OCNN ensures the best possible fit for the utilized dataset. The proposed technique was rigorously tested on two distinct datasets, achieving notably high classification accuracies. That is, the proposed OCNN for the BA-MRI dataset exhibited exceptional performance with the training accuracy of 98.94%, validation accuracy of 95.02%, and testing accuracy of 93.17%. Similarly, the proposed OCNN for the AD-MRI dataset demonstrated impressive results with achieving the training accuracy of 97.47%, validation accuracy of 95.05% and testing accuracy of 92.44%.

References

[1] Randall James Bateman, Paul Stephen Aisen, Bart De Strooper, Nick Charles Fox, Cynthia Ann Lemere, John Michael Ringman, Stephen Salloway, Reisa Ann Sperling, Manfred Windisch and Chengjie Xiong, "Autosomal-dominant Alzheimer's disease: a review and proposal for the prevention of Alzheimer's disease," Alzheimer's Research & Therapy, vol. 3, no. 1, pp. 1–13, 2011, doi: 10.1093/oed/3725923206.

[2] Rita Guerreiro and Jose Bras, "The age factor in Alzheimer's disease," Genome Medicine, vol. 7, no. 106, pp. 1–3, 2015, doi: 10.1186/s13073-015-0232-5.

[3] Benjamin Lam, Mario Masellis, Morris Freedman, Donald Todd Stuss and Sandra Elaine Black, "Clinical, imaging, and pathological heterogeneity of the Alzheimer's disease syndrome," Alzheimer's Research and Therapy, vol. 5, no. 1, pp. 1–14, 2013, doi: 10.1186/alzrt155.

[4] Luke William Bonham, Desikan Rahul Singh and Yokoyama Jennifer Sue, "The relationship between complement factor C3, APOE ε4, amyloid and tau in Alzheimer's disease," Acta neuropathologica communications, vol. 4, no. 1, p. 65, 2016, doi: 10.1186/s40478-016-0339-y.

[5] José Alberto Luchsinger and Richard Mayeux, "Dietary factors and Alzheimer's disease José," Lancet Neurology, vol. 3, no. 10, pp. 579–587, 2004, doi: 10.1016/S1474-4422(04)00870-2.

[6] Today Medical News, "Alzheimer's brain vs. normal brain." [Online]. Available: https://www.medicalnewstoday.com/articles/alzheimers-brain-vs-normal-brain

[7] Catherine Reed, Mark Belger, Dell' Agnello Grazia, Wimo Anders, Josep Maria, Argimon, Bruno Giuseppe, Dodel Richard, Josep Maria Haro, Roy W Jones and Vellas Bruno, "Caregiver Burden in Alzheimer's Disease: Differential Associations in Adult-Child and Spousal Caregivers in the GERAS Observational Study,"

Dementia and Geriatric Cognitive Disorders Extra, vol. 4, no. 1, pp. 51–64, 2014, doi: 10.1159/000358234.

[8] Natalie Susan Ryan and Martin Nicholas Rossor, "Defining and describing the pre-dementia stages of familial Alzheimer's disease," Alzheimer's Research and Therapy, vol. 3, no. 5, pp. 2010–2012, 2011, doi: 10.1186/alzrt91.

[9] Martin Dyrba, Michael Ewers, Martin Wegrzyn, Ingo Kilimann, Claudia Plant, Annahita Oswald, Thomas Meindl, Michela Pievani, Arun Lakshmanan, Andreas Fellgiebel, Massimo Filippi, Harald Hampel, Stefan Klöppel, Karlheinz Hauenstein, Thomas Kirste and Stefan, "Robust Automated Detection of Microstructural White Matter Degeneration in Alzheimer's Disease Using Machine Learning Classification of Multicenter DTI Data," PLoS ONE, vol. 8, no. 5, p. e64925, 2013, doi: 10.1371/journal.pone.0064925.

[10] Rajaram Sampath and Arunachalam Saradha, "Classification of Alzheimer's Disease Stages Exploiting an ANFIS Classifier," International Journal of Applied Engineering Research, vol. 9, no. 22, pp. 16979–16990, 2014, [Online]. Available: http://www.ripublication.com

[11] Ayşe Demirhan, Talia Miriam Nir, Artemis Zavaliangos Petropulu, Clifford Ray Jack Jr, Michael William Weiner, Matt Alan Bernstein, Paul Michael Thompson, Neda Jahanshad, and the Alzheimer's Disease Neuroimaging Initiative (ADNI), "FEATURE SELECTION IMPROVES THE ACCURACY OF CLASSIFYING ALZHEIMER DISEASE USING DIFFUSION TENSOR IMAGES," Proceedings of the IEEE International Symposium on Biomedical Imaging, vol. 176, no. 1, pp. 126–130, 2015, doi: 10.1109/ISBI.2015.7163832.FEATURE.

[12] Saman Sarraf and Ghassem Tofighi, "Classification of Alzheimer's Disease Structural MRI Data by Deep Learning Convolutional Neural Networks," arXiv preprint, 2016, doi: arXiv:1603.08631v1.

[13] Marcia Hon and Naimul Mefraz Khan, "Towards Alzheimer's Disease Classification through Transfer Learning," arXiv:1711.11117v1, 2017.

[14] Jyoti Islam and Yanqing Zhang, "Brain MRI analysis for Alzheimer's disease diagnosis using an ensemble system of deep convolutional neural networks," Brain Informatics, vol. 5, no. 2, 2018, doi: 10.1186/s40708-018-0080-3.

[15] Firouzeh Razavi, Mohammad Jafar Tarokh and Mahmood Alborzi, "An intelligent Alzheimer's disease diagnosis method using unsupervised feature learning," Journal of Big Data, vol. 6, no. 32, 2019, doi: 10.1186/s40537-019-0190-7.

[16] Sameer Mahajan, Gayatri Bangar and Nahush Kulkarni, "Machine Learning Algorithms for Classification of Various Stages of Alzheimer's Disease," International Research Journal of Engineering and Technology (IRJET), vol. 07, no. 08, pp. 817–822, 2020.

[17] Nivedhitha Mahendran, Ponnusamy Mahendran Durai Raj Vincent, Kathiravan Srinivasan and Chuan-Yu Chang, "Improving the Classification of Alzheimer's Disease Using Hybrid Gene Selection Pipeline and Deep Learning," Frontiers in Genetics, vol. 12, p. 784814, 2021, doi: 10.3389/fgene.2021.784814.

[18] Monika Sethi, Shalli Rani, Aman Singh and Juan Luis Vidal Mazón, "A CAD System for Alzheimer's Disease Classification Using Neuroimaging MRI 2D Slices," Computational and Mathematical Methods in Medicine, vol. 2022, 2022, doi: 10.1155/2022/8680737.

[19] Mohi ud din dar,Avinash Bhagat, Syed Immamul Ansarullah, Mohamed Tahar Ben Othman, Yasir Hamid, Hend Khalid Alkahtani, Inam Ullah and Habib Hamam, "A Novel Framework for Classification of Different Alzheimer's Disease Stages Using CNN Model," Electronics, vol. 12, no. 2, p. 469, 2023, doi: 10.3390/electronics12020469.

[20] Sheng Chen, Chutian Zhang, Hongjun Yang, Liang Peng, Haiqun Xie, Zeping Lv and Zeng-Guang Hou, "A Multi-Modal Classification Method for Early Diagnosis of Mild Cognitive Impairment and Alzheimer's Disease Using Three Paradigms With Various Task Difficulties," IEEE Transactions on Neural Systems and Rehabilitation Engineering, vol. 32, pp. 1477–1483, 2024, doi: 10.1109/TNSRE.2024.3379891.

[21] Duaa Mowafak Hameed and Raid Rafi Omar Al-Nima, "High-Performance Character Recognition System Utilizing Deep Convolutional Neural Networks," NTU Journal of Engineering and Technology, vol. 3, no. 4, pp. 42–51, 2024.

[22] Adnan A.Ismael, Abdulnaser A.Ahmed, Raid Rafi Omar Al-Nima, and Mohammed Khaire Hussain, "Prediction of the drainage coefficient of steeply crested inclined weirs using different neural network techniques," NTU Journal of Engineering and Technology, vol. 2, no. 4, pp. 41–44, 2023.

[23] Raid Rafi Omar Al-Nima, Saba Qasim Hasan, and Sahar Esmaiel Mahmood, "Utilizing Fingerphotos with Deep Learning Techniques to Recognize Individuals," NTU Journal of Engineering and Technology, vol. 2, no. 1, pp. 39–45, 2023.

[24] Raid Rafi Omar Al-Nima, Lubab H.Albak and Arwa H.Al-Hamdany, "Translating Sumerian Symbols into French Letters," NTU Journal of Engineering and Technology, vol. 3, no. 1, pp. 12–17, 2024.

[25] Safa N. H. Al-Moktar, Raid Rafi Omer AL-Nima, "Studying of Dual Deep Periocular Parts for Persons Recognition," NTU Journal of Engineering and Technology, vol. 2, no. 2, pp. 7–15, 2023, doi: 10.56286/ntujet.v2i2.483.

[26] Mahbub Hussain, Jordan James Bird and Faria Diego Ricardo, "A Study on CNN Transfer Learning for Image Classificatio," Advances in Intelligent Systems and Computing, vol. 840, pp. 191–202, 2019, doi: 10.1007/978-3-319-97982-3_16.

[27] Hossam Magdy Balaha, Hesham Arafat Ali, Mohamed Saraya and Mahmoud Badawy, "A new Arabic handwritten character recognition deep learning system (AHCR-DLS)," Neural Computing and Applications, vol. 33, no. 11, pp. 6325–6367, 2021, doi: 10.1007/s00521-020-05397-2.

[28] Marina Sokolova, Nathalie Japkowicz and Stan Szpakowicz, "Beyond Accuracy, F-score and ROC: a Family of Discriminant Measures for Performance Evaluation," Advances in Artificial Intelligence, pp. 1015–1021, 2006.

[29] Mohamad Zaim Awang Pon And Krishna Prakash, "Hyperparameter Tuning of Deep learning Models in Keras," Sparklinglight Transactions on Artificial Intelligence and Quantum Computing, vol. 1, no. 1, pp. 23–35, 2021.

[30] Samuel Gbashi, Obafemi Olatunji, Paul Adedeji and Nkosinathi Madushele, "Hyperparameter Optimization on CNN Using Hyperband for fault identification in wind turbine high-speed shaft gearbox bearing," International Conference on Electrical, Computer and Energy Technologies, ICECET 2023, no. November, pp. 1–7, 2023, doi: 10.1109/ICECET58911.2023.10389387.

[31] Laith Alzubaidi, Juan Santamaría, Mohammed Ali Fadhel, Muthana Al-Amidie, Laith Farhan, Jinglan Zhang, Amjad J. Humaidi, Ayad Al-Dujaili, Ye Duan and Omran Al-Shamma, "Review of deep learning: concepts, CNN architectures, challenges, applications, future directions," Journal of Big Data, vol. 8, no. 1, 2021, doi: 10.1186/s40537-021-00444-8.

[32] Saad Albawi, Tareq Abed Mohammed and Saad AL-Zawi, "Understanding of a Convolutional Neural Network," Proceedings of 2017 International Conference on Engineering and Technology, ICET 2017, pp. 1–6, 2017, doi: 10.1109/ICEngTechnol.2017.8308186.

[33] Ahmed Saeed Ibrahim Al-Obaidi, Raid Rafi Omar Al-Nima, and Tingting Han, "Interpreting Arabic Sign Alphabet by Using the Deep Learning," AIP Conference Proceedings, vol. 2862, no. 1, pp. 29–30, 2023, doi: 10.1063/5.0171428.

[34] Ihsan Evanjelist Firdausi, Irfan Mukhlash, Atyah Dhamar Syah Gama and Naufal Hidayat, "Sentiment analysis of customer response of telecommunication operator in Twitter using DCNN-SVM Algorithm," Journal of Physics: Conference Series, vol. 1490, no. 1, 2020, doi: 10.1088/1742-6596/1490/1/012071.

[35] Ernest Jeczmionek and Piotr Adam Kowalski, "Flattening layer pruning in convolutional neural networks," Symmetry, vol. 13, no. 7, pp. 1–13, 2021, doi: 10.3390/sym13071147.

[36] Wu Hao and Zhao Jinsong, "Deep convolutional neural network model based chemical process fault diagnosis," Computers & chemical engineering, vol. 115, pp. 185–197, 2018.

[37] Sagheer Abbas , Yousef Alhwaiti , Areej Fatima , Muhammad A. Khan , Muhammad Adnan Khan, Taher M. Ghazal, Asma Kanwal, Munir Ahmad and Nouh Sabri Elmitwally, "Convolutional neural network based intelligent handwritten document recognition," Computers, Materials and Continua, vol. 70, no. 3, pp. 4563–4581, 2022, doi: 10.32604/cmc.2022.021102.

[38] Weiyang Liu, Yandong Wen, Zhiding Yu and Meng Yang, "Large-Margin Softmax Loss for Convolutional Neural Networks," Proceedings of the 33rd International Conference on Machine Learning, vol. 48, 2016, [Online]. Available: http://arxiv.org/abs/1612.02295

[39] Kaggle, "Best Alzheimer MRI dataset," Accessed September 30, 2024, 2024, [Online]. Available: https://www.kaggle.com/datasets/lukechugh/best-alzheimer-mri-dataset-99-accuracy

[40] Kaggle, "Alzheimers disease MRI images," Accessed September 30, 2024, 2024, [Online]. Available: https://www.kaggle.com/datasets/shariaarfin/alzheimers-disease-mri-images?resource=download